

# Spatial quenching of a molecular charge-transfer process in a quantum fluid: The $\text{Cs}_x\text{-C}_{60}$ reaction in superfluid helium nanodroplets

Andreas W. Hauser<sup>\*,†</sup> and María Pilar de Lara-Castells<sup>‡</sup>

<sup>†</sup>*Graz University of Technology, Institute of Experimental Physics, Petersgasse 16, 8010  
Graz, Austria*

<sup>‡</sup>*Instituto de Física Fundamental, C.S.I.C., Serrano 123, E-28006 Madrid, Spain*

E-mail: andreas.w.hauser@gmail.com

The first section of this Supporting Material contains a table with parameters of our PPM model. Section 2 presents one table and three figures regarding the MCSCF+  $D_{as}$  calculations on neutral fragments, extending the appendix of the main manuscript. Section 3 contains density plots for shorter and larger distances than what is shown in the main manuscript. Section 4 compares the CDFT results of various functionals for the charge-neutral interaction of the triplet  $\text{Cs}_2$  dimer with a  $\text{C}_{60}$  fullerene.

# Contents

1	Pairwise Potential Model for the He-C <sub>60</sub> Interaction	3
2	Dispersion-corrected MCSCF calculations of Neutral States	3
3	Additional He-DFT contour plots	8
4	CDFT results for triplet Cs <sub>2</sub> with various functionals	9
	References	9

# 1 Pairwise Potential Model for the He-C<sub>60</sub> Interaction

Table 1: Parameters defining the dispersionless and dispersion contributions to the He/C<sub>60</sub> interaction energy using the pairwise additive potential model proposed in this work.

Dispersionless interaction energy				
$R_c / \text{\AA}$	$A / \text{eV}$	$\alpha / \text{\AA}^{-1}$	$\beta / \text{\AA}^{-2}$	$\gamma_R$
18.0	1191.268	4.182	-0.110	-0.83
Dispersion energy				
	$C_6^X / \text{eV} \cdot \text{\AA}^6$	$C_8^X / \text{eV} \cdot \text{\AA}^8$	$\beta^X / \text{\AA}^{-1}$	$\gamma_A$
X=C	9.897	1975.2	3.487	-0.49
X=He	0.678	0.266	4.763	-

As mentioned in the appendix of the main manuscript, a pairwise potential model (PPM) has been developed to fit ab-initio interaction energies for the He-C<sub>60</sub> interaction. Table 1 lists the PPM parameters while Figure 1 plots the PPM total and dispersion energies as a function of the distance from the He atom to the C<sub>60</sub> mass center, comparing them with those obtained at DFT-SAPT level by Hesselmann and Korona.<sup>1</sup> Notice that the PPM reproduces both total and dispersion He/C<sub>60</sub> interaction energies rather accurately.

## 2 Dispersion-corrected MCSCF calculations of Neutral States

As mentioned in the appendix of the main manuscript, state-average (two-state) MCSCF calculations have been performed to describe the van-der-Waals neutral Cs-C<sub>60</sub> and Cs<sub>2</sub>-C<sub>60</sub> interactions, with the latter in the electronic triplet and singlet states. The Cs and Cs<sub>2</sub> species were located along the C<sub>3</sub> axis of fullerene, with the Cs–Cs axis oriented perpendicularly to the C<sub>3</sub> axis. For Cs we used the same basis set as in the B97M-V calculations (see Section 2.1 of the main manuscript) but employed the polarized correlation-consistent double- $\zeta$  basis sets of Dunning and collaborators<sup>2</sup> for carbon atoms. To define the MCSCF active space we

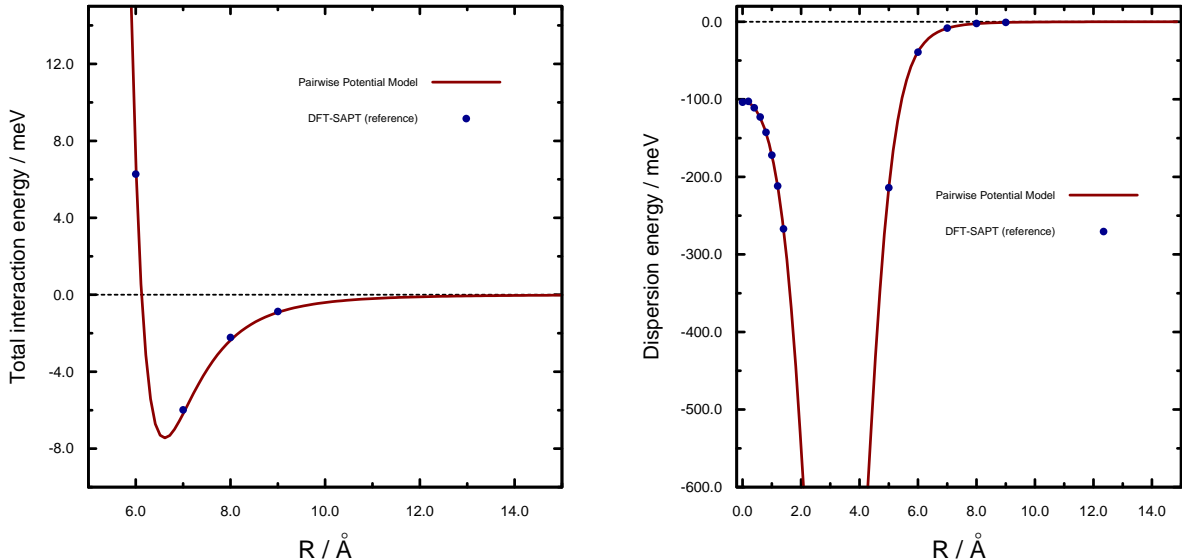


Figure 1: He/C<sub>60</sub> total (left panel) and dispersion (right panel) interaction energies as a function of the distance from the He atom to the C<sub>60</sub> mass center, as obtained with the DFT-SAPT approach by Hesselmann and Korona<sup>1</sup> and our pairwise potential model. The He atom is located along the C<sub>3</sub> symmetry axis of fullerene.

considered the 5s orbitals from the Cs and Cs<sub>2</sub> species along with frontier  $\pi$ -type molecular orbitals of the C<sub>60</sub> fragment. Although the active space was rather restrictive, it allowed us to obtain the two states correlating asymptotically to Cs<sub>x</sub>+C<sub>60</sub> and Cs<sub>x</sub><sup>+</sup>+C<sub>60</sub><sup>-</sup> fragments at the long-range potential region. It was tested that the wave-function of the state correlating to neutral Cs<sub>x</sub>/C<sub>60</sub> fragments is strongly dominated by a single reference configuration.

For the Cs<sub>2</sub>(triplet)-C<sub>60</sub> complex, Figure 2 shows the two MCSCF potential energy curves as a function of the distance, denoted  $R$ , between the Cs<sub>2</sub> and fullerene mass centers. Note that the two states in this figure have radically different character. The ground state describes the strong Coulomb interaction between a negatively charged fullerene and a positively charged cesium dimer. In contrast, the excited state corresponds to the interaction of a neutral Cs<sub>2</sub> with a fullerene (physisorption) and correlates asymptotically to Cs<sub>2</sub>+C<sub>60</sub>. In the long-range region (i.e. at distances larger than about 7 Å), our Mulliken population analysis showed that the Cs<sub>2</sub> monomer is kept neutral in the state correlating to Cs<sub>2</sub>+C<sub>60</sub>.

At distances shorter than about 7 Å, however, the excited state was identified with an excited charge-transfer state via redistribution of the electronic charge localized in the fullerene fragment. Hence, the neutral  $\text{Cs}_x + \text{C}_{60}$  potential energy curve was extrapolated at the potential wall region by fitting to an exponential function. From Figure 2 it can be seen that the crossing between ionic and neutral potential energy curves at MCSCF level takes place at long distances (ca. 8 Å), as it is typically found for interactions governed by the harpoon mechanism.<sup>3</sup> Moreover, preliminary calculations adding dynamical correlation energy contributions to the MCSCF interaction energies show that the crossing region moves to intermolecular distances even larger (ca. 10.5 Å).

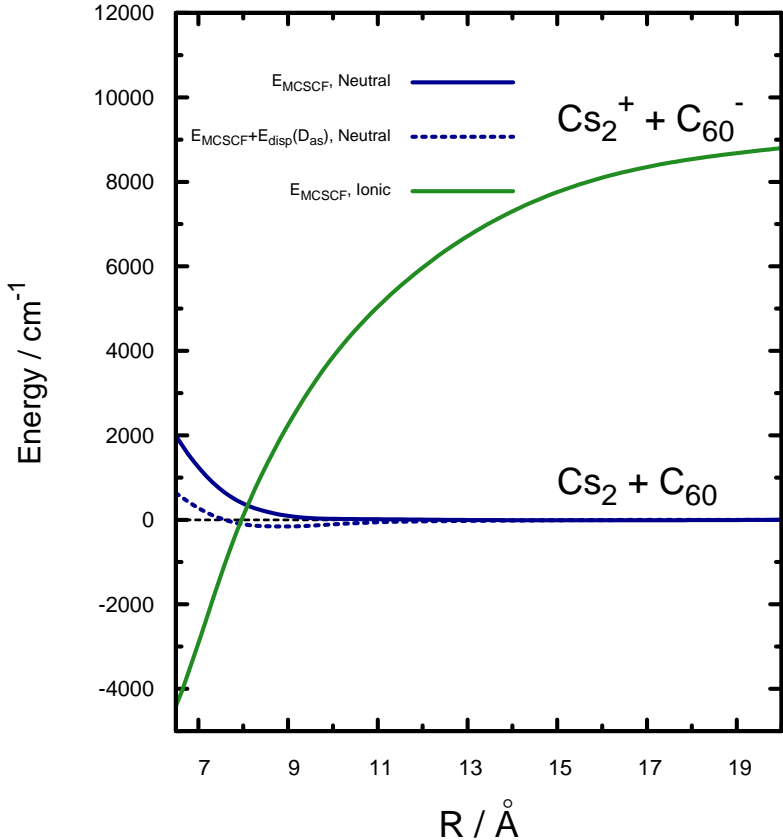


Figure 2:  $\text{Cs}_2(\text{triplet})\text{-C}_{60}$  interaction energies as a function of the distance between the corresponding mass centers along the  $\text{C}_3$  symmetry axis, obtained with the MCSCF method. The  $\text{Cs}_2$  molecule is oriented perpendicularly to the  $\text{C}_3$  symmetry axis of fullerene.

An obvious flaw of the MCSCF approach is the lack of dynamical correlation. To include these contributions (see also appendix of the main manuscript) we performed CCSD(T) calculations for the Cs/C<sub>6</sub>H<sub>6</sub> and Cs<sub>2</sub>(triplet,singlet)/C<sub>6</sub>H<sub>6</sub> complexes. In the next step, the correlation CCSD(T) energies were fitted to the effective interatomic pairwise  $D_{as}$  functional.<sup>4,5</sup> Figure 3 compares the calculated CCSD(T) correlation energies with those fitted via the functional  $D_{as}$ . The root-mean-square errors of these fits were below 1 meV and 0.1 meV for the Cs<sub>2</sub>(triplet)/benzene and Cs/benzene complexes, respectively. In contrast with the original  $D_{as}$  approach,<sup>4</sup> where the parameters were fitted for a given training sets of molecules, we tune the  $D_{as}$  function for the considered system (fullerene) using a small representative cluster (benzene). This procedure has been validated for the adsorption of noble-gas and metal atoms on carbon-based substrates.<sup>6-8</sup> Finally, the functional  $D_{as}$  was used to estimate the dispersion Cs-C<sub>60</sub> and Cs<sub>2</sub>-C<sub>60</sub> energies. As can be seen in Figure 2, the van der Waals Cs<sub>2</sub>(triplet)-C<sub>60</sub> interaction potential becomes attractive when the long-range dispersion correction is taken into consideration. As an additional test, preliminary calculations were carried out by adding dynamical correlation contributions to the MCSCF interaction energies via multi-state second-order multi-reference perturbation theory (MS-CASPT2), as implemented in the MOLPRO program.<sup>9</sup> These two-state MS-CASPT2 calculations were carried out for the Cs<sub>2</sub>(singlet)-C<sub>60</sub> complex and the same multi-configurational space as in the precedent MCSCF computations: MCSCF+ $D_{as}$  and MS-CASPT2 potential energy curves for the neutral Cs<sub>2</sub>-C<sub>60</sub> complex agreed very well to each other, with energy differences below 7% at the well region. However, further SAPT-DFT calculations for the Cs<sub>2</sub>-C<sub>60</sub> complex indicated that both our MCSCF+ $D_{as}$  and MS-CASPT2 procedures might underestimate the attractive van-der-Waals-type interaction (e.g., by a factor of 1.4 at a distance of 12 Å).

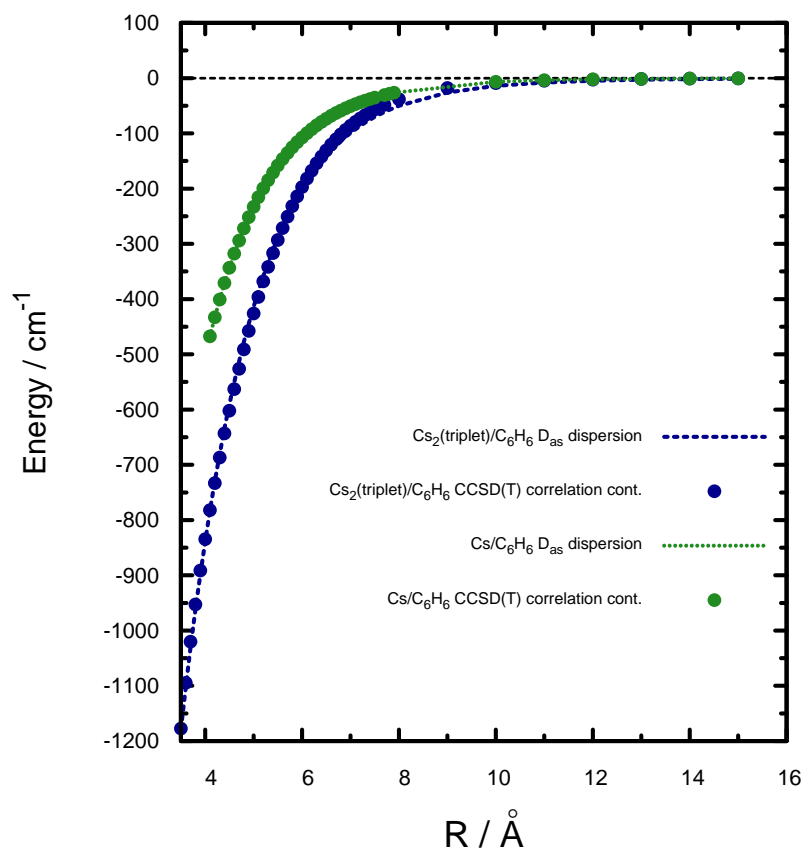


Figure 3:  $\text{Cs}/\text{C}_6\text{H}_6$  and  $\text{Cs}_2(\text{triplet})/\text{C}_6\text{H}_6$  interaction energies as functions of the distance between the corresponding mass centers along the  $\text{C}_6$  symmetry axis, as obtained with the CCSD(T) method and the parametrization of the  $D_{as}$  functional. The  $\text{Cs}_2$  molecule is oriented perpendicularly to the  $\text{C}_6$  symmetry axis.

### 3 Additional He-DFT contour plots

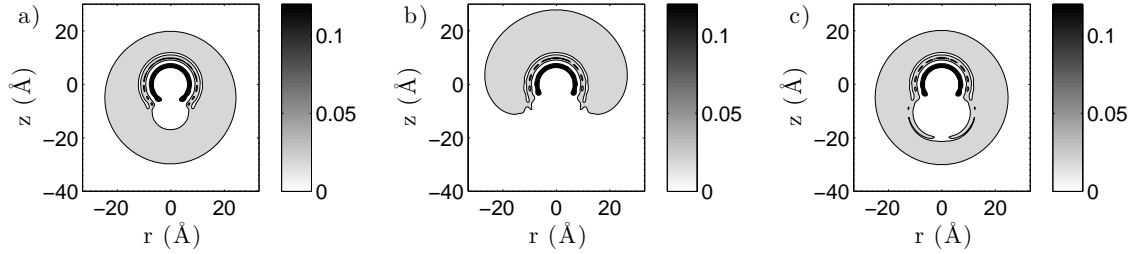


Figure 4: Contour plots of the helium density for a distance of 10 Å between the fullerene and (a) a single Cs atom, (b) the triplet Cs<sub>2</sub> dimer in collinear configuration, (c) the triplet Cs<sub>2</sub> dimer in T-shaped (c) configuration. The density is plotted in units of Å<sup>-3</sup>. Note that the bulk value for the density of liquid helium is 0.02185 atoms per Å<sup>3</sup>.

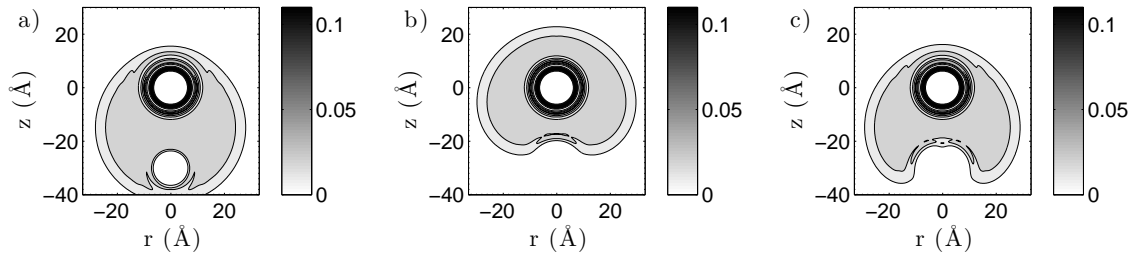


Figure 5: Contour plots of the helium density for a distance of 30 Å between the fullerene and (a) a single Cs atom, (b) the triplet Cs<sub>2</sub> dimer in collinear configuration, (c) the triplet Cs<sub>2</sub> dimer in T-shaped (c) configuration. The density is plotted in units of Å<sup>-3</sup>. Note that the bulk value for the density of liquid helium is 0.02185 atoms per Å<sup>3</sup>.

## 4 CDFT results for triplet $\text{Cs}_2$ with various functionals

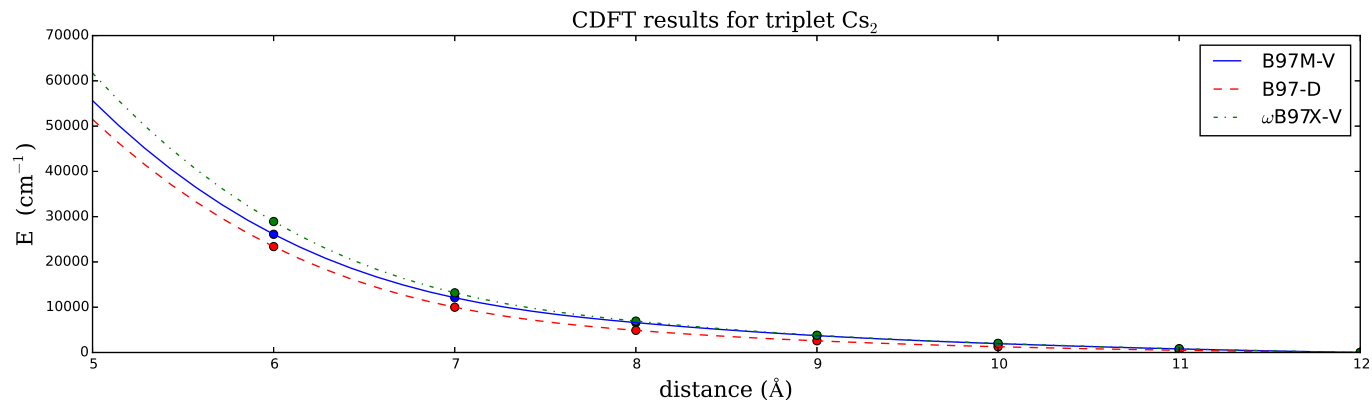


Figure 6: Interaction of a fullerene with a triplet  $\text{Cs}_2$  dimer in T-shaped configuration, calculated with three different functionals.

## References

- (1) Hesselmann, A.; Korona, T. *Phys. Chem. Chem. Phys.* **2011**, *13*, 732.
- (2) Woon, D. E.; Dunning, T. H. *The Journal of Chemical Physics* **1994**, *100*.
- (3) Magee, J. L. *J. Chem. Phys.* **1940**, *8*, 687.
- (4) Pernal, K.; Podeszwa, R.; Patkowski, K.; Szalewicz, K. *Phys. Rev. Lett.* **2009**, *103*, 263201.
- (5) Podeszwa, R.; Pernal, K.; Patkowski, K.; Szalewicz, K. *J. Phys. Chem. Lett.* **2010**, *1*, 550–555.
- (6) de Lara-Castells, M. P.; Stoll, H.; Civalleri, B.; Causà, M.; Voloshina, E.; Mitrushchenkov, A. O.; Pi, M. *J. Chem. Phys.* **2014**, *141*, 151102.
- (7) de Lara-Castells, M. P.; Mitrushchenkov, A. O.; Stoll, H. *J. Chem. Phys.* **2015**, *143*, 102804.

- (8) de Lara-Castells, M. P.; Bartolomei, M.; Mitrushchenkov, A. O.; Stoll, H. *J. Chem. Phys.* **2015**, *143*, 194701.
- (9) Werner, H. J.; Knowles, P. J.; Knizia, G.; Manby, F. R.; Schütz, M.; Celani, P.; Korona, T.; Lindh, R.; Mitrushchenkov, A. O.; Rauhut, G.; et al., MOLPRO, version 2012.1, a package of *ab initio* programs, see <http://www.molpro.net>.